

Report Number 11/61

Asymptotic solution of a model for bilayer organic diodes and solar
cells

by

Giles Richardson, Colin Please, and James Kirkpatrick



Oxford Centre for Collaborative Applied Mathematics
Mathematical Institute
24 - 29 St Giles'
Oxford
OX1 3LB
England

ASYMPTOTIC SOLUTION OF A MODEL FOR BILAYER ORGANIC DIODES AND SOLAR CELLS

GILES RICHARDSON*, COLIN PLEASE†, AND JAMES KIRKPATRICK‡

Abstract. The current voltage characteristics of an organic semiconductor diode made by placing together two materials with dissimilar electron affinities and ionisation potentials is analysed using asymptotic methods. An intricate boundary layer structure is examined. We find that there are three regimes for the total current passing through the diode. For reverse bias and moderate forward bias the dependency of the voltage on the current is similar to the behaviour of conventional inorganic semiconductor diodes predicted by the Shockley equation and are governed by recombination at the interface of the materials. There is then a narrow range of currents where the behaviour undergoes a transition. Finally for large forward bias the behaviour is different with the current being linear in voltage and is primarily controlled by drift of charges in the organic layers. The size of the interfacial recombination rate is critical in determining the small range of current where there is rapid transition between the two main regimes. The extension of the theory to organic solar cells is discussed and the analogous current voltage curves derived in the regime of interest.

Key words. Shockley model, drift diffusion, asymptotic analysis, photovoltaic

AMS subject classifications. 82D37, 34E05, 35B40, 78A57

1. Introduction. Organic materials are promising materials for many semiconducting applications, for example light emitting diodes [1], field effect transistors[2], sensors [3] and solar cells [4]. They are already widely applied in the xerographic industry [5]. Their attraction is that they enable devices to be designed with similar properties to those made from traditional semiconductors, such as silicon and gallium arsenide, but at a fraction of the cost. This is primarily due to high throughput processing techniques such as roll to roll printing and screen printing of organic inks. A timely and exciting application of this technology, which is the main motivator for this paper, is that such devices provide the possibility of very cheap large-scale solar cells. There are many companies inching closer to making organic photovoltaic diodes with energy efficiencies sufficient for commercialisation [6]. As a first step in analysing such solar cell behaviour it is necessary to understand the “dark current” when the device is not illuminated and acts as a simple diode. At the moment much progress in developing these devices is by trial and error and an in-depth understanding of organic semiconductor devices and how they differ from their inorganic counterparts would provide a method to enhance the speed of device improvement.

The operation of crystalline, inorganic solar cells is a well developed area [7]. In a traditional silicon device a p-n junction is created by doping part of the device with donor atoms (to make a n-type region) while the other part is doped with acceptor atoms (to make a p-type region). The resulting electric potential created across the device creates an electric field in the relatively narrow depletion layer straddling the interface where the two regions meet. The p-type region is typically doped to a much higher level than the n-type region and as a consequence the current is effectively governed by diffusion of minority carriers (electrons) in the p-type region. When

*School of Mathematics, University of Southampton, Southampton SO17 1BJ, UK (g.richardson@soton.ac.uk)

†School of Mathematics, University of Southampton, Southampton SO17 1BJ, UK(c.p.please@soton.ac.uk)

‡OCCAM, University of Oxford, 24 - 29 St Giles’ Oxford, OX1 3LB, UK (kirkpatrick@maths.ox.ac.uk).

used as a solar cell the light is absorbed within the device to simultaneously create electron-hole pairs and these charges are very mobile and hence easily separated by the electric field.

Organic semiconductors differ in that they are not usually doped. They can be divided into two broad classes of behaviour dependent on the electron affinity and the ionisation potential of the material. In materials with a small electron affinity (deep empty energy levels) electrons are more stable than holes and such materials are therefore classed as electron acceptors. In contrast, in materials with a large ionisation potential (shallow filled energy levels) holes are more stable than electrons such that these materials are known as electron donors. Junctions in organic semiconducting devices are made by placing donor and acceptor materials next to each other. The aim of this paper is to understand in detail how the resulting interface between materials with different electron affinities and ionisation potentials is capable of producing a diode with current voltage characteristics similar to those of a traditional pn junction. When used as solar cells there is a further significant difference in behaviour. Light absorption produces localised, strongly bound excitation states, similar to an electron and hole, but which cannot readily separate spontaneously into free charges as happens in the case of traditional inorganic materials. However, these excitation states can be broken at the interface by the significant changes in the ionisation potential and electron affinity. Hence the interface plays a role similar to the electric field in the depletion layer of a conventional device.

A major problem that needs to be surmounted, in order to produce efficient organic solar cells, is the short timescale on which the excitation states recombine (return to their un-excited state). As these excited states move by diffusion an efficient device requires that the distance the excited state can diffuse before recombining (the exciton diffusion length) is not significantly smaller than the thickness of material necessary to absorb a significant percentage of sunlight (the optical thickness). Unfortunately optical thicknesses (around 200nm) are typically much larger than exciton diffusion lengths (around 10nm) so a planar device of around 200nm absorbs most of the light but loses most of the absorbed energy as the excited states recombine in the bulk before reaching the donor-acceptor interface, whereas an extremely thin planar device (of around 10nm) converts most of the absorbed energy into free charges but absorbs very little light. In either case these are poor solar cells. The current solution is to use complex morphologies for the acceptor and donor materials, resulting in a convoluted interface with a high surface area for a given volume. Rightly most studies so far [8, 9, 10] have concentrated on the crucial role of this convoluted morphology to determine efficiency, but so far as we are aware there has been little work addressing the fundamental differences in operation of conventional and organic semiconducting diodes, namely the importance of an interface between materials with different electron affinities. We want to concentrate on the role of interface and to understand the basic electronic operation of an organic diode, and therefore exclude the role of morphology by looking at bilayer devices where a layer of a certain thickness of one material is deposited over another one (the device is planar and the interface is flat). In this context we are aware of, as yet unpublished work, by Brinkman *et al.* [11], that adopts a broadly similar approach. Thin bilayer devices are not simply of academic interest, they can, when stacked to make a multiple heterojunction device, provide high power conversion photovoltaic cells [12]. In this study we concentrate on the diode behaviour of a solar cell. The role the interface plays in separating photo-generated excitation states into charge carriers is extremely important, but confuses

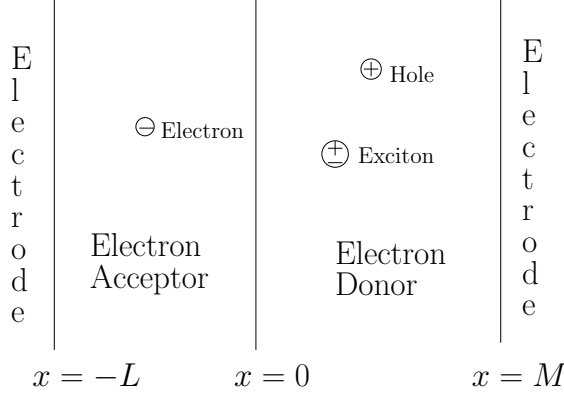


FIG. 2.1. *The geometry of the solar-cell.*

the underlying physical phenomena of transport and recombination, so that we do not initially include it in our model but rather leave it until §4 until describing how the generation and subsequent separation (at the semiconductor interface) of excitation states modifies the current voltage curve in the regime of physical interest.

An interesting aspect of the behaviour of organic diodes (both in conventional use and as solar cells) is that the current flow through them can vary by over seven orders of magnitude with relatively small changes in applied voltage as they move from forward to reverse bias (see, for example, [13]). This makes numerical solution of any realistic model of the device extremely challenging. Here we shall adopt an asymptotic approach which is ideally suited to such problems and which has the added advantage of giving simple analytic formulae for most of the current-voltage curve. This analysis is nontrivial and gives rise to rarely encountered asymptotic phenomena such as boundary layers with thickness determined by the boundary conditions applied on the outer problem.

In this paper we solve the current transport equations for a diode formed of a planar interface between two slabs of organic materials, one electron donating and one electron accepting. By exploiting physically relevant limiting values of the parameters we distinguish three regimes for the current voltage characteristics. The first is for relatively small currents (in reverse bias or in moderate forward bias) where the current voltage curve is similar to that of an ideal diode, which gives the current as a constant plus an exponential function of the voltage [7]. The second is a narrow range of medium sized currents where the behaviour changes character smoothly and the third region is for large currents (in hard forward bias) where the current voltage relationship is linear.

2. Equations. The main processes which are going on in an organic diode are charge transport in the bulk of both donor and acceptor materials, and charge recombination at the interface between the two materials. A reasonable mathematical description of such devices must therefore both describe the behaviour of charge inside the material and at the interface between the two materials.

A schematic for a simple bilayer organic photovoltaic device lying between $-L < x < M$ with the interface at $x = 0$ between the electron acceptor material ($-L < x < 0$) and donor material ($0 < x < M$) is shown in figure 2.1.

2.1. Current continuity equations in each material. Many complex models of charge transport in organic semiconductors exist in the literature including multiple trapping models [14], Gaussian disorder models [15], and atomistic models [16]. In this paper the motion of electrons and holes through the semiconductors is modelled by simple drift diffusion, allowing for the possibility that the diffusion coefficient depends upon electric field, while accounting for the different electron affinities of the materials via spatially dependent ionisation potentials (see for example [7]). These equations are coupled to the Poisson equation for the electric potential. Since charge generation occurs only at the interface between donor and acceptor we shall assume that there is no significant generation or recombination in the bulk of the semiconductors. The resulting one-dimensional equations are therefore:

$$\frac{\partial n}{\partial t} + \frac{\partial \mathcal{F}_n}{\partial x} = 0, \quad (2.1)$$

$$\frac{\partial p}{\partial t} + \frac{\partial \mathcal{F}_p}{\partial x} = 0, \quad (2.2)$$

$$\frac{\partial}{\partial x} \left(\varepsilon \frac{\partial \phi}{\partial x} \right) = q(n - p), \quad (2.3)$$

$$\mathcal{F}_n = -D_n \left(\frac{\partial n}{\partial x} + \frac{1}{kT} n \frac{\partial \psi_n}{\partial x} \right), \quad (2.4)$$

$$\mathcal{F}_p = -D_p \left(\frac{\partial p}{\partial x} - \frac{1}{kT} p \frac{\partial \psi_p}{\partial x} \right), \quad (2.5)$$

$$\psi_n = \mu_n(x) - q\phi, \quad (2.6)$$

$$\psi_p = \mu_p(x) - q\phi, \quad (2.7)$$

where, \mathcal{F}_n is the flux of electrons, \mathcal{F}_p is the flux of holes, n is the charge density of electrons, p of holes, ϕ is the electric potential, and the material properties are given by μ_p the ionisation potential, μ_n the electron affinity, k Boltzmann's constant, T the temperature, ε the permittivity, and q the charge on an electron. We shall term the functions ψ_n and ψ_p the energy levels of the lowest unoccupied molecular orbital (LUMO) and highest unoccupied molecular orbital (HOMO), respectively while noting that there is some dispute about the correct notation for these quantities with some authors applying them to μ_n and μ_p instead.¹ The functions ψ_n and ψ_p are what would typically be sketched in the band diagram of a semiconductor device and in conventional materials would be termed the conduction and valence band edges, respectively. Electrons in the LUMO experience a force down gradients in ψ_n while holes in the HOMO experience a force up gradients in ψ_p . At the interface the jumps in ψ_n and ψ_p mean that electrons are attracted into the acceptor from the donor while holes experience a force in the opposite direction. Rough sketches of the band diagram of an organic diode in both forward and reverse bias are made in figure 2.2. Note that the total current density J can be expressed as the difference of hole and electron fluxes thus:

$$J = q(\mathcal{F}_p - \mathcal{F}_n). \quad (2.8)$$

¹These functions are also sometimes termed the electrochemical potentials; this is confusing since the more standard definition of the electrochemical potentials includes an entropic contribution which is a function (typically a log) of the species concentration.

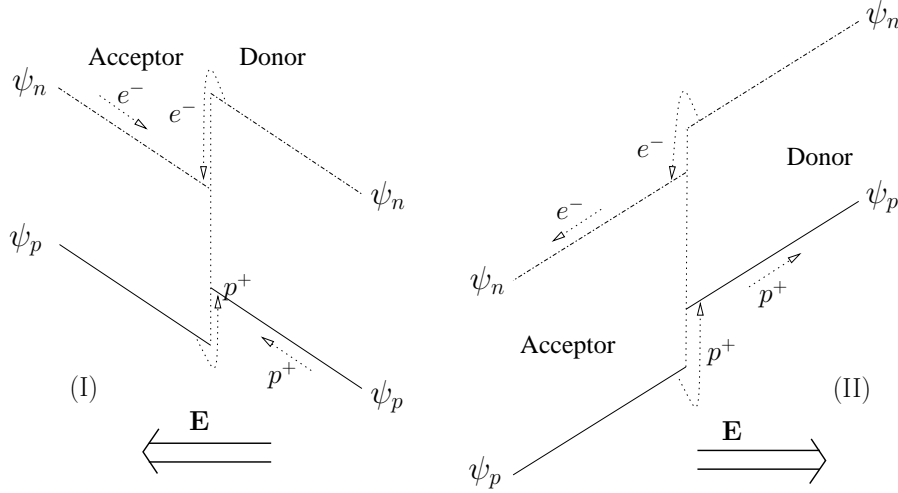


FIG. 2.2. Sketches of the band diagram for organic diodes in (I) forward bias and (II) reverse bias showing the energy levels of the HOMO by solid lines and LUMO edge by dot-dash lines. At the semiconductor interface the jump in energy levels leads to migration of electrons from the donor to the acceptor and migrations of holes in the reverse direction. In forward bias the electric field tilts the LUMO and HOMO levels so that electrons flow toward the interface in the acceptor and holes flow towards the interface in the donor; this leads to high concentrations of these two species at the interface and hence high recombination. In contrast, in reverse bias, the electric field tilts the LUMO and HOMO levels the other way so that electrons in the acceptor and holes in the donor migrate away from the interface. Since recombination of the majority carriers (electrons in the acceptor and holes in the donor) at the interface typically controls current flow in the diode much higher current flows can be achieved in forward bias than in reverse bias.

In inorganic materials the diffusion coefficients are usually taken as constant or as functions of the material and temperature. However, unlike the movement of free charges in an inorganic semiconductor, transport in an organic material is primarily through charges jumping between nearby trap states. There is considerable interest in modelling this transport process and one of the simplest descriptions is provided by the Poole-Frenkel model [7, 9, 8] where the diffusivities D_n and D_p are taken to be functions of the local electric field. The form taken is usually

$$D_n \left(\frac{\partial \phi}{\partial x} \right) = D_{n,0} \exp \left(\gamma \left| \frac{\partial \phi}{\partial x} \right|^{1/2} \right), \quad D_p \left(\frac{\partial \phi}{\partial x} \right) = D_{p,0} \exp \left(\gamma \left| \frac{\partial \phi}{\partial x} \right|^{1/2} \right)$$

where $D_{n,0}$, $D_{p,0}$ and γ are constants. More complex models can be derived accounting, for example, for a density of trap states in the material. Such a model results in the fraction of charges which are free to move being dependent on the charge density itself [14], so that the diffusivity depends directly on the charge density [17]. We do not include such effects here.

The model above allows for general structures in the device but here we are interested in modelling two adjacent regions each of a uniform material, therefore we assume that the electron affinity and ionisation potential are constant in each material so that

$$\mu_n = \begin{cases} \mu_{n-} & \text{in } x < 0 \\ \mu_{n+} & \text{in } x > 0 \end{cases}, \quad \mu_p = \begin{cases} \mu_{p-} & \text{in } x < 0 \\ \mu_{p+} & \text{in } x > 0 \end{cases}. \quad (2.9)$$

where μ_{n-} , μ_{n+} , μ_{p-} and μ_{p+} are constants.

2.2. Organic-organic Interface. Two key features must be taken into consideration at the interface between two organic semiconductors. Firstly there is a jump in electron affinity and the ionisation potential and in order to preserve equilibrium at the interface, this results in jumps in electron and hole concentrations. Localised interface charged states have been postulated at the interface (*e.g.* [9]) but here we ignore such states and explicitly neglect the effect of any surface dipoles or charges so that the electric potential and displacement field are both continuous across the interface. Therefore we can write the jump conditions

$$[\phi]_{x=0}, \quad \left[\varepsilon \frac{\partial \phi}{\partial x} \right]_{x=0} = 0, \quad (2.10)$$

$$[\log n]_{x=0} = - \left[\frac{\mu_n}{kT} \right]_{x=0}, \quad [\log p]_{x=0} = \left[\frac{\mu_p}{kT} \right]_{x=0}. \quad (2.11)$$

The second important feature of the organic-organic interface is that this is where recombination and generation occur in the device. Note that because the ionisation potential and electron affinity differ by a large amount the materials are nearly insulators and there is negligible recombination of electrons and holes in the bulk of the device. Electrons from the acceptor side are able to recombine with holes from the donor side (at the interface) and vice versa. The resulting recombination flux R_b results in jumps in the electron and hole current fluxes. This is central to the behaviour of this type of solar cell - this mechanism allows the electron current in the acceptor to turn into a hole current in the donor. We expect the recombination rate to depend on the product of electron densities at $x = 0_-$ and the holes at $x = 0_+$, namely $(n|_{x=0_-})(p|_{x=0_+})$ (or alternatively $(n|_{x=0^+})(p|_{x=0^-})$). A general expression could be derived but, because of the conditions in (2.11), the electron densities at $x = 0_-$ are directly proportional to those at $x = 0_+$ and similarly for holes. This allows us a certain freedom in choosing the form of the interface recombination rate in terms of the charge densities on either side of the interface. Since we expect that the most important role is played by majority carriers (electrons in the acceptor and holes in donor) we express the recombination flux in terms of those densities only. Hence we take

$$[\mathcal{F}_n]_{x=0} = -R_b (n|_{x=0^-}, p|_{x=0^+}), \quad (2.12)$$

$$[\mathcal{F}_p]_{x=0} = -R_b (n|_{x=0^-}, p|_{x=0^+}). \quad (2.13)$$

2.3. Existence of an equilibrium state and boundary conditions. Before considering what are sensible boundary conditions we consider the existence of an equilibrium state of (2.1)-(2.7). An equilibrium state is a steady state where both the electron and hole fluxes are both simultaneously zero, that is: $\mathcal{F}_n^{equil} \equiv 0$ and $\mathcal{F}_p^{equil} \equiv 0$. Therefore from (2.4 - 2.5) with (2.11) it follows that n and p take the form

$$n = A \exp \left(-\frac{1}{kT} \psi_n(x) \right), \quad p = B \exp \left(\frac{1}{kT} \psi_p(x) \right),$$

for some constants A and B . We note that this solution has a special property which we find by multiplying the equilibrium concentrations to give

$$np = AB \exp \left(-\frac{1}{kT} (\mu_n(x) - \mu_p(x)) \right) \quad (2.14)$$

The right-hand side of (2.14) only depends on material properties and so we introduce the notation

$$np = N_D^2 \exp\left(-\frac{1}{kT} (\mu_n(x) - \mu_p(x))\right) \quad (2.15)$$

where we write $AB = N_D^2$ and this relates to the density of states in the material.

The equilibrium condition in the dark occurs when no applied potential is present. Since different metals are typically used to contact the electron and donor materials the potential difference across the device consists of both the *applied* potential V and a *built-in* potential V_{bi} which results from the difference of workfunctions of the two metallic contacts (if the same metal is used for both contacts then $V_{bi} = 0$). At equilibrium, when by definition $V = 0$, the boundary conditions for the (total) potential is $\phi|_{x=-L} = V_{bi}/2$ and $\phi|_{x=M} = -V_{bi}/2$ then

$$\begin{aligned} n &= A \exp\left(-\frac{1}{kT} \left(\mu_{n-} - q\frac{V_{bi}}{2}\right)\right)\Big|_{x=-L}, \quad p = B \exp\left(\frac{1}{kT} \left(\mu_{p-} - q\frac{V_{bi}}{2}\right)\right)\Big|_{x=-L}, \\ n &= A \exp\left(-\frac{1}{kT} \left(\mu_{n+} + q\frac{V_{bi}}{2}\right)\right)\Big|_{x=M}, \quad p = B \exp\left(\frac{1}{kT} \left(\mu_{p+} + q\frac{V_{bi}}{2}\right)\right)\Big|_{x=M}. \end{aligned} \quad (2.16)$$

These equations show the role of the built-in voltage: it allows large concentrations of electrons (or holes) at the contacts. The diffusion arising from these large charge densities must be balanced by a drift term, therefore a built-in voltage allows an equilibrium state to exist with non-zero electric field.

The Recombination Rate. The need for an equilibrium also partly determines the functional form that the recombination at the interface must take. Since both electron and hole fluxes must be zero at equilibrium the recombination rate must also be zero in this case. It is natural to therefore write R_b as a product with

$$R_b = K(n|_{x=0-}, p|_{x=0+}) \left((n|_{x=0-})(p|_{x=0+}) - N_D^2 \exp\left(-\frac{\mu_{n-} - \mu_{p+}}{kT}\right) \right),$$

and $K(n, p) > 0$. Here the recombination can be seen as composed of two parts: the recombination of electrons and holes (proportional to $n|_{x=0-}p|_{x=0+}$) and a thermal generation part proportional to the intrinsic charge density ($-N_D^2 \exp\left(-\frac{\mu_{n-} - \mu_{p+}}{kT}\right)$). Since other properties also depend on the difference of electron affinity in the acceptor and the ionisation potential in the donor we define this quantity as the pseudo band-gap $E_g = \mu_{n-} - \mu_{p+}$. Notice that this is not a band gap in the conventional sense: usually a band gap is a property of a single material such as the difference between the electron affinity and the ionisation potential, whereas in this case the pseudo band-gap relates to the pair of materials. However, because it defines the temperature dependence of the thermal generation of charges, it plays a very similar role to the band gap in a traditional semiconductor. Writing the recombination at the interface in the form of equation (2.17) allows us considerable freedom in the choice of the function K . It could be a constant, giving us direct recombination, or it could be proportional to the inverse of the charge densities, giving a Shockley-Read-Hall recombination. It could also depend on the electric field or on temperature. Henceforth we shall assume that this term has the form of a Shockley-Reid-Hall recombination term writing:

$$R_b = K_0 \left(\frac{(n|_{x=0-})(p|_{x=0+}) - N_D^2 \exp(-E_g/(kT))}{1 + u_1 n|_{x=0-} + u_2 p|_{x=0+}} \right), \quad (2.17)$$

which can be interpreted as recombination controlled by a single intermediate state at the interface. If different forms of the recombination were used, the form of some of the parameters in the asymptotic analysis, which follow, would change but this would not change the general thrust of the model.

Boundary Conditions. At the boundaries it is typically assumed that there are many surface states so that local equilibrium is always retained. This is obviously compatible with the need to have an equilibrium solution (2.16). The resulting boundary conditions at the contacts with the electrodes are

$$np|_{x=-L} = N_D^2 \exp\left(-\frac{1}{kT}(\mu_{n-} - \mu_{p-})\right), \quad (2.18)$$

$$np|_{x=M} = N_D^2 \exp\left(-\frac{1}{kT}(\mu_{n+} - \mu_{p+})\right). \quad (2.19)$$

The final boundary conditions at the contacts come from imposing the potential and from jump conditions relating to the electron concentration. These conditions take the form

$$\begin{aligned} n &= \tilde{n}_- \exp\left(-\frac{E_g}{2kT} + \frac{qV_{bi}}{2kT}\right) \quad \text{and} \quad \phi = \frac{V + V_{bi}}{2} \quad \text{on} \quad x = -L, \\ p &= \frac{N_D^2}{\tilde{n}_-} \exp\left(-\frac{E_g}{2kT} + \frac{qV_{bi}}{2kT}\right) \quad \text{and} \quad \phi = -\frac{V + V_{bi}}{2} \quad \text{on} \quad x = M. \end{aligned} \quad (2.20)$$

where the value of $p|_{x=M}$ is chosen in order to ensure that condition (2.16) is satisfied. This condition on p is equivalent to the assumption of Ohmic contacts (namely that the Fermi level in the semiconductor is assumed equal to the work function of the metal) resulting in an electron and hole density which is independent of the applied potential. Without loss of generality the boundary conditions on the potential have been chosen to be antisymmetric in order to simplify later calculations.

2.4. Nondimensionalisation . In order to analyse the problem we introduce nondimensional variables, indicated by the superscript *. This allows us to consider physically relevant ranges for the resulting dimensional parameters. For most of the variables the scalings are straightforward. We take

$$\begin{aligned} x &= Lx^*, & t &= \frac{L^2}{\bar{D}}t^*, & n &= \Pi_0 n^*, & p &= \Pi_0 p^*, \\ \psi_p &= \frac{\mu_{p-} + \mu_{p+}}{2} + kT\psi_p^*, & \phi &= \frac{kT}{q}\phi^*, & \varepsilon &= \bar{\varepsilon}\varepsilon^*, \\ \psi_n &= \frac{\mu_{n-} + \mu_{n+}}{2} + kT\psi_n^*, & \mathcal{F}_n &= \frac{\bar{D}\Pi_0}{L}\mathcal{F}_n^*, & \mathcal{F}_p &= \frac{\bar{D}\Pi_0}{L}\mathcal{F}_p^*, & J &= \frac{\bar{D}\Pi_0 q}{L}J^*, \end{aligned} \quad (2.21)$$

where the constant $\bar{\varepsilon}$ is a typical permittivity, \bar{D} is a typical diffusivity and we choose the typical electron/hole concentration, Π_0 , to be given by

$$\Pi_0 = N_D \exp\left(-\frac{E_g}{2kT}\right)$$

which has a role similar to the intrinsic carrier concentration used in inorganic semiconductor theory.

On substituting the above into (2.1)-(2.7) and (2.17)-(2.20) we obtain the following dimensionless equations:

$$\frac{\partial n^*}{\partial t^*} + \frac{\partial \mathcal{F}_n^*}{\partial x^*} = 0, \quad (2.22)$$

$$\frac{\partial p^*}{\partial t^*} + \frac{\partial \mathcal{F}_p^*}{\partial x^*} = 0, \quad (2.23)$$

$$\frac{\partial}{\partial x^*} \left(\varepsilon^* \frac{\partial \phi^*}{\partial x^*} \right) = \frac{1}{\lambda^2} (n^* - p^*), \quad (2.24)$$

$$\mathcal{F}_n^* = -\kappa_n \exp \left(\nu \left| \frac{\partial \phi^*}{\partial x^*} \right|^{1/2} \right) \left(\frac{\partial n^*}{\partial x^*} - n^* \frac{\partial \phi^*}{\partial x^*} \right), \quad (2.25)$$

$$\mathcal{F}_p^* = -\kappa_p \exp \left(\nu \left| \frac{\partial \phi^*}{\partial x^*} \right|^{1/2} \right) \left(\frac{\partial p^*}{\partial x^*} + p^* \frac{\partial \phi^*}{\partial x^*} \right), \quad (2.26)$$

with the jump conditions on the interface

$$[\phi^*]_{x^*=0} = 0, \quad \left[\varepsilon^* \frac{\partial \phi^*}{\partial x^*} \right]_{x^*=0} = 0, \quad [\log n^*]_{x^*=0} = -H_n, \quad [\log p^*]_{x^*=0} = H_p, \quad (2.27)$$

$$[\mathcal{F}_n^*]_{x^*=0} = [\mathcal{F}_p^*]_{x^*=0} = -2\delta \left(\frac{n^*|_{x^*=0^-} p^*|_{x^*=0^+} - 1}{\lambda^2 \theta + U n^*|_{x^*=0^-} + (1-U) p^*|_{x^*=0^+}} \right), \quad (2.28)$$

and the boundary conditions:

$$\begin{aligned} n^*|_{x^*=-1} &= \tilde{N}_- \exp \left(\frac{\Phi_{bi}}{2} \right), \quad p^*|_{x^*=-1} = \frac{1}{\tilde{N}_-} \exp \left(-\frac{\Phi_{bi}}{2} - H_p \right), \quad \phi^*|_{x^*=-1} = \frac{\Phi + \Phi_{bi}}{2}, \\ p^*|_{x^*=m} &= \frac{1}{\tilde{N}_-} \exp \left(\frac{\Phi_{bi}}{2} \right), \quad n^*|_{x^*=m} = \tilde{N}_- \exp \left(-\frac{\Phi_{bi}}{2} - H_n \right), \quad \phi^*|_{x^*=m} = -\frac{\Phi + \Phi_{bi}}{2}. \end{aligned} \quad (2.29)$$

The total current density is

$$J^* = \mathcal{F}_p^* - \mathcal{F}_n^*, \quad (2.30)$$

and the dimensionless energies of the LUMO and HOMO are

$$\left. \begin{aligned} \psi_n^* &= -\frac{H_n}{2} - \phi^* \\ \psi_p^* &= -\frac{H_p}{2} - \phi^* \end{aligned} \right\} \text{ in } x < 0 \quad \text{and} \quad \left. \begin{aligned} \psi_n^* &= \frac{H_n}{2} - \phi^* \\ \psi_p^* &= \frac{H_p}{2} - \phi^* \end{aligned} \right\} \text{ in } x > 0. \quad (2.31)$$

The dimensionless parameters in the problem are defined by

$$\begin{aligned} \kappa_n &= \frac{D_{n0}}{\bar{D}}, \quad \theta = \frac{1}{\lambda^2 N_D (u_1 + u_2)} \exp \left(\frac{-E_g}{2kT} \right), \quad \lambda = \frac{1}{L} \left(\frac{\varepsilon kT}{q^2 \Pi_0} \right)^{1/2}, \\ \kappa_p &= \frac{D_{p0}}{\bar{D}}, \quad \tilde{N}_- = \frac{\tilde{n}_-}{N_D}, \quad \Phi = \frac{q}{kT} V, \\ \nu &= \gamma \left(\frac{kT}{qL} \right)^{1/2}, \quad U = \frac{u_1}{u_1 + u_2}, \quad \delta = \frac{LK_0}{2\bar{D}(u_1 + u_2)}, \\ m &= \frac{M}{L}, \quad H_n = \frac{\mu_{n+} - \mu_{n-}}{kT}, \quad H_p = \frac{\mu_{p+} - \mu_{p-}}{kT}, \end{aligned} \quad (2.32)$$

$$\Phi_{bi} = \frac{q}{kT} V_{bi}.$$

We use existing physical data to consider the size of the various parameters. A typical electron/hole concentration is, according to [9], $\Pi_0 = O(10^{22})\text{m}^{-3}$, device width is about $L = O(10^{-7})\text{m}$, the permittivity $\bar{\varepsilon}$ is similar to the permittivity of free space $\varepsilon_0 = 8.85 \times 10^{-12}\text{A sV}^{-1}\text{m}^{-1}$. Buxton and Clarke [8] take $\gamma = 5 \times 10^{-4}\text{m}^{1/2}\text{V}^{-1/2}$. The charge on an electron is $q = 1.6 \times 10^{-19}\text{C}$. Using these numbers we estimate the parameters in the model as follows:

$$\lambda \approx O(1), \quad \gamma \approx O(1), \quad H_n \gtrsim 50, \quad H_p \gtrsim 50. \quad (2.33)$$

and will therefore exploit the largeness of H_n and H_p in our analysis. Other parameters in the problem are less well documented and part of the motivation for the analysis done here is to identify how the general behaviour depends on these values. For most parameters we shall assume that they do not take extreme values, however we find that the dependency of the voltage on the current is critically altered by the value of δ . Unless δ is very small the voltage-current characteristic does not have the behaviour observed in devices. We shall therefore make the assumption that δ is very small in our analysis.

Note that from hereon, for simplicity we drop the superscript * notation from the dimensionless variables.

2.5. Simplifications: large jumps in electron affinity, no Poole-Frenkel behaviour and an antisymmetric device . Using materials that are strong electron donors and electron acceptors (*i.e.* $H_n \gg 1$ and $H_p \gg 1$) means that the concentration of holes in the acceptor material and of electrons in the donor material are extremely small. In a silicon device these minority carriers are responsible for carrying much of the current, whereas in an organic device their role is insignificant. This is because it is possible for the majority carriers in the donor (holes) to recombine with the majority carriers in the acceptor (electrons) at the interface between the two organic semiconductors. This corresponds to the major simplification that the electron concentration in the donor material and the hole concentration in the acceptor material of an organic diode are both zero

$$p \equiv 0 \quad \text{in } x < 0, \text{ and } \quad n \equiv 0 \quad \text{in } x > 0,$$

which is justified by the extremely small sizes of $\exp(-H_p)$ and $\exp(-H_n)$. We also make three other simplifications: that the Poole-Frenkel behaviour is insignificant, that the device is at steady state and that the device is perfectly antisymmetric, corresponding to

$$\nu = 0, \quad \varepsilon_- = \varepsilon_+, \quad \kappa_p = \kappa_n, \quad \tilde{N}_- = 1, \quad m = 1 \quad (2.34)$$

and by suitable choice of $\bar{\varepsilon}$ and \bar{D} that specifically

$$\varepsilon_- = \varepsilon_+ = 1 \quad \kappa_p = \kappa_n = 1. \quad (2.35)$$

By assuming that the device is anti-symmetric we can deduce that $n(-x) = p(x)$ (for $0 < x < 1$) and that the electric potential distribution is antisymmetric $\phi(-x) = -\phi(x)$. These simplifications allow a straightforward analysis of the problem avoiding much of the algebraic complexity and reveals the general structure of the solution for practical applications. In particular, the neglect of the Poole-Frenkel effect simplifies the analysis without making major qualitative changes to the device behaviour. We discuss its inclusion in the conclusions.

After making these simplifications and considering only half of the antisymmetric device the model takes the form:

$$\left. \begin{aligned} \frac{\partial p}{\partial x} + p \frac{\partial \phi}{\partial x} &= -J \\ \frac{\partial^2 \phi}{\partial x^2} &= -\frac{p}{\lambda^2} \end{aligned} \right\} \quad \text{in} \quad 0 < x < 1, \quad (2.36)$$

$$J = -\frac{2\delta(p^2|_{x=0} - 1)}{(\lambda^2\theta + p|_{x=0})}, \quad (2.37)$$

$$p|_{x=1} = \exp\left(\frac{\Phi_{bi}}{2}\right), \quad \phi|_{x=1} = -\frac{\Phi + \Phi_{bi}}{2}, \quad \phi|_{x=0} = 0. \quad (2.38)$$

3. Asymptotic solution of simplified model. We now attempt to find approximate solutions to the simplified model. In doing this we shall exploit the fact that δ is an extremely small number in practical devices. We justify this assumption by noting that in efficient devices the current varies by many orders of magnitude as the potential across the device is varied from hard reverse bias to hard forward bias (in, for example, the devices fabricated by Potscavage *et al.* [13] there is a variation in the magnitude of the current by a factor of about 10^6 from hard reverse bias to hard forward bias). As we shall demonstrate it is only possible to achieve such large variations in the current if recombination at the interface between the two semiconductors is very difficult (*i.e.* $\delta \ll 1$). If the recombination is easy the device acts predominantly as an Ohmic resistor. All other parameters are taken to be order one except for the voltage Φ and the current J which we vary in order to find the relationship between Φ and J . In fact we will need to consider different regimes based on the sizes of these two parameters, relative to δ . We remark that the dimensionless built-in potential $\Phi_{bi} = qV_{bi}/(kT)$ is typically large in practice but that in comparison to $\log(1/\delta)$ we still expect it to be small. Furthermore, we assert that, under these circumstances, investigating the distinguished limit $\Phi_{bi} = O(1)$ still yields valid results.

We start by defining the new quantities:

$$N_a = \frac{1}{\lambda^2}, \quad \hat{J} = \frac{J}{2\lambda^2}, \quad (3.1)$$

and substituting for p (in terms of ϕ) in (2.36b) from (2.36c) enables us to rewrite equations (2.36)-(2.38) in the form:

$$\frac{\partial^3 \phi}{\partial x^3} + \frac{\partial \phi}{\partial x} \frac{\partial^2 \phi}{\partial x^2} = 2\hat{J} \quad \text{in} \quad 0 < x < 1, \quad (3.2)$$

$$\phi = 0 \quad \text{and} \quad \hat{J} = -\delta \frac{\phi_{xx}^2 - N_a^2}{\theta - \phi_{xx}} \quad \text{on} \quad x = 0, \quad (3.3)$$

$$\phi = -\frac{\Phi + \Phi_{bi}}{2} \quad \text{and} \quad \frac{\partial^2 \phi}{\partial x^2} = -\exp\left(\frac{\Phi_{bi}}{2}\right) N_a \quad \text{on} \quad x = 1. \quad (3.4)$$

We now proceed to solve this ODE in the limits of small and large currents to obtain the relevant current-voltage characteristics.

3.1. Small current limit . When the current is small, the system lies close to the equilibrium solution in which drift and diffusion components of the current

density are large compared to the total current density and are almost in balance. Physically this is a regime in which the current in the bulk of the semiconductors is small and is determined by the rate of recombination at the interface. Formally we investigate the distinguished asymptotic limit $\hat{J} = O(\delta)$ and $\Phi + \Phi_{bi} = O(1)$ but note that the approximate solution we derive is asymptotically valid provided $\hat{J} \ll 1$; this is equivalent to requiring $-\Phi \ll \log(1/\delta)$. Hence we look for an asymptotic solution to (3.2)-(3.4) of the form

$$\phi = \phi_0 + \delta\phi_1 + \dots, \quad \hat{J} = \delta\hat{J}_1 + \dots,$$

Substituting this ansatz into (3.2)-(3.4) yields the following problem at leading order:

$$\frac{\partial^3 \phi_0}{\partial x^3} + \frac{\partial \phi_0}{\partial x} \frac{\partial^2 \phi_0}{\partial x^2} = 0 \quad \text{in } x > 0, \quad (3.5)$$

$$\phi_0 = 0 \quad \text{and} \quad \hat{J}_1 = -\frac{\phi_{0xx}^2 - N_a^2}{\theta - \phi_{0xx}} \quad \text{on } x = 0, \quad (3.6)$$

$$\phi_0 = -\frac{\Phi + \Phi_{bi}}{2} \quad \text{and} \quad \frac{\partial^2 \phi_0}{\partial x^2} = -N_a \exp\left(\frac{\Phi_{bi}}{2}\right) \quad \text{on } x = 1. \quad (3.7)$$

Integrating (3.5) once and applying the boundary conditions (3.7a-b) gives the relation

$$\frac{\partial^2 \phi_0}{\partial x^2} = -N_a \exp\left(-\frac{\Phi}{2}\right) \exp(-\phi_0). \quad (3.8)$$

This is all we need in order to derive the current-voltage curve since it allows us to evaluate $\phi_{0,xx}|_{x=0}$, using the fact that $\phi_0|_{x=0} = 0$, and hence to find \hat{J}_1 from (3.6b). This yields

$$\hat{J}_1 = \frac{2N_a^2 \sinh(\Phi/2)}{N_a + \theta \exp(\Phi/2)} \quad (3.9)$$

Thus this part of the current voltage curve is given, on substituting for \hat{J} and N_a from (3.1), by

$$J \sim 4\delta \frac{\sinh(\Phi/2)}{1 + \lambda^2 \theta \exp(\Phi/2)}. \quad (3.10)$$

The solution for ϕ_0 . Solving for ϕ_0 from (3.8), together with the boundary conditions (3.6a) and (3.7a), yields a solution that takes either the form

$$\phi_0 = -2 \log\left(\frac{\sinh(p)}{\sinh(p \pm Ax)}\right), \quad \text{where } A \text{ and } p \text{ satisfy} \quad (3.11)$$

$$\frac{\sinh^2 p}{\sinh^2(p \pm A)} = \exp\left(\frac{\Phi + \Phi_{bi}}{2}\right) \quad \text{and} \quad \frac{2A^2}{\sinh^2(p \pm A)} = N_a \exp\left(\frac{\Phi_{bi}}{2}\right). \quad (3.12)$$

or the form

$$\phi_0 = -2 \log\left(\frac{\sin q}{\sin(q \pm Bx)}\right), \quad \text{where } B \text{ and } q \text{ satisfy} \quad (3.13)$$

$$\frac{\sin^2 q}{\sin^2(q \pm B)} = \exp\left(\frac{\Phi + \Phi_{bi}}{2}\right) \quad \text{and} \quad \frac{2B^2}{\sin^2(q \pm B)} = N_a \exp\left(\frac{\Phi_{bi}}{2}\right). \quad (3.14)$$

Thus if $N_a \exp\left(\frac{\Phi_{bi}}{2}\right) < 2$ the appropriate form from the solution is (3.11)-(3.12) while if $N_a \exp\left(\frac{\Phi_{bi}}{2}\right) > 2$ the appropriate form from the solution is (3.13)-(3.14).

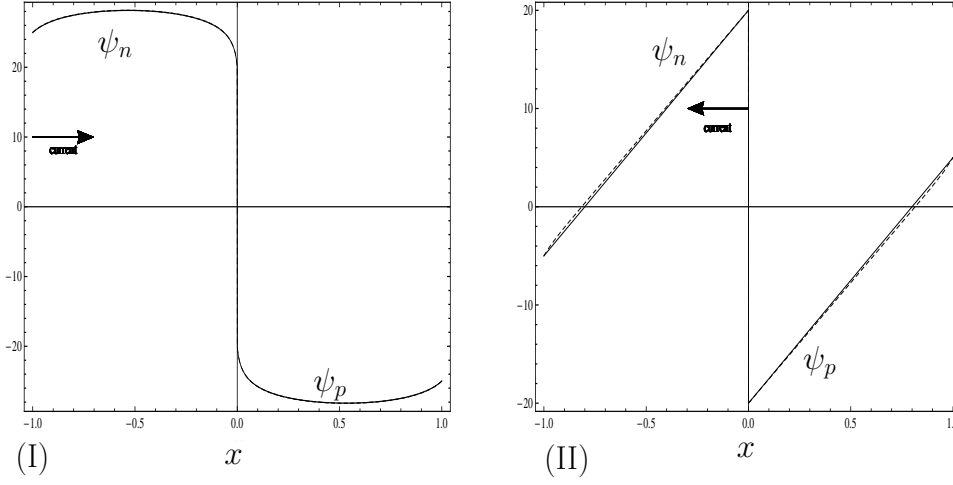


FIG. 3.1. Diagrams showing the dimensionless energies of the LUMO, ψ_n , in $x < 0$ and the HOMO, ψ_p , in $x > 0$. Both diagrams assume a pseudo band gap E_g of 40 (1 eV) and $\Phi_{bi} = 12$ with $\lambda = 1$. However in (I) $\Phi = -22$ corresponding to a device in forward bias while in (II) $\Phi = 38$ corresponding to a device in reverse bias. Shown are solutions calculated directly from the numerical solution to (3.12) (dotted lines) and ones derived from the approximate solutions (3.19), in forward bias, and (3.16), in reverse bias (solid lines).

Reverse Bias. In hard reverse bias when the applied voltage is much greater than Φ_{bi} equation (3.10) reduces to:

$$\hat{J}_1 \sim \frac{N_a^2}{\theta} \quad \text{as } \Phi \rightarrow \infty, \quad (3.15)$$

This corresponds to the reverse saturation current in a traditional Shottky diode. It is also possible to look at the potential distribution in these conditions. This is done by solving equation (3.12) and approximating the hyperbolic arc cosecant function by a logarithm. The potential can then be written as:

$$\phi_0 \sim -\frac{\Phi}{2}x. \quad (3.16)$$

A physical picture is easy to glean: in reverse bias some charges are generated thermally at the interface and are being removed by a constant electric field. Since in our model the thermally generated current is voltage independent, the reverse current saturates. Figure 3.1(II) shows this approximate solution and the corresponding numerical solution for the dimensionless energy levels of the LUMO and HOMO (ψ_n and ψ_p , respectively) as defined in (2.31).

Forward bias. In forward bias, the potential is large and negative and in this case equation (3.10) can be approximated by an exponential:

$$\hat{J}_1 \sim -N_a \exp\left(-\frac{\Phi}{2}\right) \quad \text{as } \Phi \rightarrow -\infty. \quad (3.17)$$

this situation is very similar to the standard solution to the Shockley equation where the forward bias current is written as $J \propto \exp(-\Phi/n)$, where n is the so called ideality factor. The ideality factor we obtain here is therefore equal to 2. This is because in

the limit of large charge density, and in an antisymmetric configuration, the Shockley Read Hall recombination term varies as the charge density. Since the charge density at the interface is proportional to $\exp(\Phi/2)$, the ideality factor is 2. If we had used bare recombination, where the recombination flux is proportional to charge density squared, we would have obtained an ideality factor of 1.

By assuming that both $-\Phi \gg 1$ it is, again, possible to obtain approximate expressions for the potential distribution both in an exponentially narrow layer in the immediate vicinity of the junction (*i.e.* for $x = O(\exp(-|\Phi|/4))$) and away from it (*i.e.* for $x = O(1)$).² Rather than write down both these expressions we write down a uniformly valid asymptotic expression for the potential throughout $0 \leq x \leq 1$

$$\phi_0 \sim -2 \log \left(\frac{\pi \xi_2 e^{-|\Phi|/4}}{\sin(\pi(x + \xi_2 e^{-|\Phi|/4}))} \right), \quad (3.18)$$

where $\xi_2 = \sqrt{\frac{2}{N_a}}$ and $\xi_2 \ll 1$

This form of the solution is appropriate to study both the potential distribution at equilibrium and in forward bias. An example showing the dimensionless energy levels of LUMO and HOMO in forward bias (calculated from (3.19) and (2.31)) is shown in figure 3.1(I). Here, as the bias is increased, the levels bend further and further at the interface, increasing the charge density. The increase in charge density drives a greater current through the device. At forward bias electrons are injected in the donor, holes are injected in the acceptor and they annihilate at the interface.

3.1.1. The large current large potential asymptotics $-\hat{J} = O(\log(1/\delta))$, $-\Phi = O(\log(1/\delta))$. As the voltage becomes larger in magnitude (in forward bias), the charge density at the interface increases exponentially as does the current. This increase in current can only continue in quasi static equilibrium so long as the increase in drift current towards the interface can be matched by a similar increase in diffusion away from the interface. Such a diffusion relies on draining the bulk of the semiconductor away from the interface of charges and this cannot be sustained indefinitely. For sufficiently large voltage the current is controlled by the transport in the bulk of the device.

Here we write $\hat{J} = \log(1/\delta)\hat{J}_*$ where $\hat{J}_* < 0$ and $-\hat{J}_* = O(1)$. In terms of this new variable the steady state equations are

$$\frac{\partial^3 \phi}{\partial x^3} + \frac{\partial \phi}{\partial x} \frac{\partial^2 \phi}{\partial x^2} = -2|\hat{J}_*| \log\left(\frac{1}{\delta}\right) \quad \text{in } x > 0, \quad (3.19)$$

$$\phi = 0 \quad \text{and} \quad |\hat{J}_*| = \frac{\delta}{\log(1/\delta)} \frac{\phi_{xx}^2 - N_a^2}{\theta - \phi_{xx}} \quad \text{on } x = 0, \quad (3.20)$$

$$\phi = -\frac{\Phi + \Phi_{bi}}{2} \quad \text{and} \quad \frac{\partial^2 \phi}{\partial x^2} = -N_a \exp(\Phi_{bi}/2) \quad \text{on } x = 1. \quad (3.21)$$

In order to study this problem we need to investigate the boundary layer about $x = 0$ whose width is found by balancing the right hand side of (3.20b) with the modulus of the current density $|\hat{J}_*|$.

²The asymptotic expansion remains valid provided $|\delta \hat{J}_1| \ll 1$ which is equivalent to the condition $|\Phi| \ll 2 \log(N_a/\delta)$.

Inner region (II). The role of this boundary layer region is to match the charge density to the recombination condition. This is a region, in which a quasi-equilibrium holds, with a high concentration of charge and is reminiscent of an inversion layer. Immediately adjacent to the semiconductor interface on $x = 0$ we introduce the scaled variable η which is related to x via

$$x = \frac{\delta^{1/2}}{(\log(1/\delta))^{1/2}} \eta,$$

In terms of this new variable the equations and boundary conditions (3.19)-(3.20) become

$$\frac{\partial^3 \phi}{\partial \eta^3} + \frac{\partial \phi}{\partial \eta} \frac{\partial^2 \phi}{\partial \eta^2} = O \left(\delta^{3/2} \log \left(\frac{1}{\delta} \right)^{-1/2} \right) \quad \text{in } \eta > 0, \quad (3.22)$$

$$\phi = 0 \quad \text{and} \quad |\hat{J}_*| = -\frac{\phi_{\eta\eta}^2 - \delta^2 (\log(1/\delta))^{-2} N_a^2}{\phi_{\eta\eta} - \delta (\log(1/\delta))^{-1} \theta} \quad \text{on } \eta = 0. \quad (3.23)$$

Expanding ϕ as follows

$$\phi^{(II)} = \phi_2^{(II)} + \dots,$$

and substituting into (3.22)-(3.23) yields the leading order problem

$$\begin{aligned} \frac{\partial^3 \phi_2^{(II)}}{\partial \eta^3} + \frac{\partial \phi_2^{(II)}}{\partial \eta} \frac{\partial^2 \phi_2^{(II)}}{\partial \eta^2} &= 0, \\ \phi_2^{(II)} &= 0 \quad \text{and} \quad \frac{\partial^2 \phi_2^{(II)}}{\partial \eta^2} = -|\hat{J}_*| \quad \text{on } \eta = 0, \end{aligned}$$

with solution

$$\phi_2^{(II)} = 2 \log \left(1 + \left| \frac{\hat{J}_*}{2} \right|^{1/2} \eta \right). \quad (3.24)$$

We now require to match this to an outer region on the $O(1)$ lengthscale. However, in order to do this, we need to introduce an intermediate inner region and match across this region from the inner to the outer. In this intermediate inner region (as in the inner region) a quasi-equilibrium exists.

Intermediate inner region (I). Here we rescale about the interface on $x = 0$ by introducing the new variable ξ , defined by

$$x = \frac{\xi}{\log(1/\delta)}, \quad \left(\xi = \delta^{1/2} (\log(1/\delta))^{1/2} \eta \right)$$

in terms of which (3.19) can be rewritten as

$$\frac{\partial^3 \phi}{\partial \xi^3} + \frac{\partial \phi}{\partial \xi} \frac{\partial^2 \phi}{\partial \xi^2} = -\frac{2|\hat{J}_*|}{\log \left(\frac{1}{\delta} \right)^2}.$$

Matching to the leading order solution in the inner region we see that the expansion for ϕ proceeds, in powers of δ , as follows:

$$\phi^{(I)} = \log \left(\frac{1}{\delta} \right) - \log \left(\log \left(\frac{1}{\delta} \right) \right) + \phi_2^{(I)} + \dots. \quad (3.25)$$

Proceeding to $O(1)$ in the expansion of (3.25) gives the following equation for $\phi_2^{(I)}$:

$$\frac{\partial^3 \phi_2^{(I)}}{\partial \xi^3} + \frac{\partial^2 \phi_2^{(I)}}{\partial \xi^2} \frac{\partial \phi_2^{(I)}}{\partial \xi} = 0,$$

with solution

$$\phi_2^{(I)} = C + 2 \log(\sinh(M\xi)),$$

where the constants C and M are determined by the matching conditions. Matching to the leading order inner solution implies

$$\phi_2^{(I)} \sim 2 \log \left(\left| \frac{\hat{J}_*}{2} \right|^{1/2} \xi \right) \quad \text{as } \xi \rightarrow 0,$$

and thus implies that

$$\phi_2^{(I)} = \log \left| \frac{\hat{J}_*}{2} \right| - 2 \log M + 2 \log(\sinh(M\xi)). \quad (3.26)$$

where the remaining constant M is determined by matching to the outer region.

The outer region (o). Finally we get to the outer region in which we solve (3.19) with boundary condition (3.21) (where $x = O(1)$). This is the region where drift dominates: the semiconductor has a uniform charge density and a constant electric field dictated by the current. By matching to the solution in the intermediate inner region it becomes apparent that the asymptotic expansion of the solution in the outer region takes the form

$$\begin{aligned} \phi^{(o)} &= \log \left(\frac{1}{\delta} \right) \phi_0^{(o)} + \log \left(\log \left(\frac{1}{\delta} \right) \right) \phi_1^{(o)} + \phi_2^{(o)} + \dots, \\ \Phi + \Phi_{bi} &= \log \left(\frac{1}{\delta} \right) \Xi_0 + \log \left(\log \left(\frac{1}{\delta} \right) \right) \Xi_1 + \Xi_2 + \dots. \end{aligned}$$

Substituting into (3.19) leads to the leading order equation $\phi_0^{(o)}{}_{xx} = 0$ with solution

$$\phi_0^{(o)} = Ax + B.$$

where A and B are constants. Proceeding to $O(\log(1/\delta))$ in (3.19) and (3.21b) gives

$$\phi_2^{(o)}{}_{xx} = -\frac{2|\hat{J}_*|}{A} \quad \text{and} \quad \phi_2^{(o)}{}_{xx}|_{x=1} = -N_a \exp(\Phi_{bi}/2)$$

from which we conclude that $A = 2|\hat{J}_*|/(N_a \exp(\Phi_{bi}/2))$ so that

$$\phi_0^{(o)} = \frac{2|\hat{J}_*|}{N_a \exp(\Phi_{bi}/2)} x + B. \quad (3.27)$$

Proceeding to $O(\log(1/\delta) \log(\log(1/\delta)))$ and to $O(\log(\log(1/\delta)))$ leads to the result that

$$\phi_1^{(o)} = K, \quad \Xi_1 = -2K, \quad (3.28)$$

where K is a constant.

Matching and the large current current-voltage curve. Matching between (3.25), the solution in the intermediate inner region, as $\xi \rightarrow \infty$ and (3.27)-(3.28), that in the outer region, as $x \rightarrow 0$, at the two leading orders serves to determine $B = 1$ and $K = -1$ so that the two leading order terms in the outer solution are uniquely determined as

$$\phi_0^{(o)} = \frac{2|\hat{J}_*|}{N_a \exp(\Phi_{bi}/2)}x + 1, \quad \phi_1^{(o)} = -1. \quad (3.29)$$

Applying the boundary condition (3.21a) to this solution allows us to determine the two leading terms in the potential drop across the cell as

$$\Xi_0 = -\frac{4|\hat{J}_*|}{N_a \exp(\Phi_{bi}/2)} - 2, \quad \text{and} \quad \Xi_1 = 2. \quad (3.30)$$

Thus this part of the current voltage curve is given, on substituting for \hat{J} and N_a from (3.1), by

$$J \sim \frac{1}{2} \left((\Phi + \Phi_{bi}) + 2 \log(1/\delta) - 2 \log \left(\log \left(\frac{1}{\delta} \right) \right) \right) \exp(\Phi_{bi}/2). \quad (3.31)$$

Notably J depends linearly with Φ , the result of Ohmic dissipation in the semiconductor bulk which becomes significant for sufficiently large forward biased currents.

Matching the intermediate inner to the outer to find M . As $\xi \rightarrow \infty$ the solution (3.26) for $\phi_2^{(I)}$ (the second order intermediate inner) has the far field behaviour

$$\phi_2^{(I)} \sim 2M\xi \quad \text{as} \quad \xi \rightarrow \infty.$$

This term matches onto x -dependence of the leading order outer solution as $x \rightarrow 0$. Looking at (3.29) we can thus identify

$$M = \frac{|\hat{J}_*|}{N_a \exp(\Phi_{bi}/2)}$$

so that $\phi_2^{(I)}$ is uniquely determined as

$$\phi_2^{(I)} = \log \left| \frac{\hat{J}_*}{2} \right| - 2 \log \left(\frac{|\hat{J}_*|}{N_a \exp(\Phi_{bi}/2)} \right) + 2 \log \left(\sinh \left(\frac{|\hat{J}_*|}{N_a \exp(\Phi_{bi}/2)} \xi \right) \right).$$

3.1.2. The current-voltage curves for small and large J . In (3.10) and (3.31) we have derived asymptotic expressions for the current-voltage curve in the limits of small and large currents, respectively. An example of the results obtained using these expressions is plotted in figure 3.2 for $\Phi_{bi} = 4$, $\delta = e^{-8}$, $\lambda = 1$ and $\theta = 0.4$ (where the solid lines represent the results of the small J asymptotics and the dashed line that of the large J asymptotics). As alluded to previously the small current asymptotics indicate the current saturates in hard reverse bias with $J \sim 2\delta/(\lambda^2\theta)$ as $\Phi \rightarrow +\infty$ (see figure 3.2b) and that it grows exponentially with $-\Phi$ in hard forward bias with $J \sim -2\delta \exp(-\Phi/2)$ as $\Phi \rightarrow +\infty$ (again see figure 3.2b). However for significantly large negative potentials (when $\Phi + \Phi_{bi}$ becomes comparable with $-2 \log(1/\delta)$) the exponential growth ceases and is replaced by linear growth of the form $J \sim \frac{1}{2}((\Phi + \Phi_{bi}) + 2 \log(1/\delta)) \exp(\Phi_{bi}/2)$ for potentials $\Phi + \Phi_{bi}$ significantly

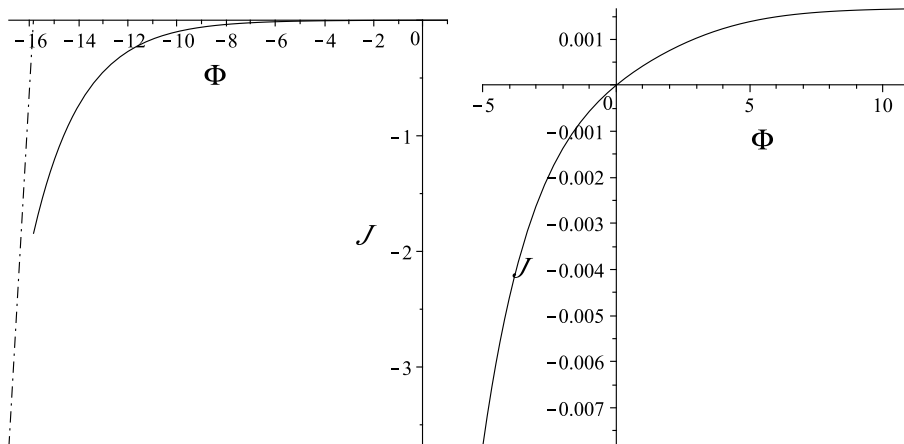


FIG. 3.2. Typical current-voltage curves derived from the low-current asymptotics (3.10) - shown by solid curve - and from the high current asymptotics (3.31) - shown by a dashed curve. Here $\Phi_{bi} = 4$, $\delta = e^{-8}$, $\lambda = 1$ and $\theta = 0.4$. The left panel shows both low- and high- current current-voltage curves. Not shown is the intermediate current approximation for which we have no explicit expression. The right panel shows only the low current approximation.

less than $-2\log(1/\delta)$. This linear growth is shown by the dashed line in figure 3.2a. Notably there is a mismatch between the asymptotic expressions for the current-voltage curve in the vicinity of $\Phi + \Phi_{bi} = -2\log(1/\delta)$. In order to explain this mismatch we need to consider one more asymptotic regime, namely the intermediate current asymptotics (see below).

3.1.3. The intermediate current asymptotics: $\hat{J} < 0$ with $\hat{J} = O(1)$, $\Phi + \Phi_{bi} = -2\log(1/\delta) + O(1)$. In order to complete the asymptotic description of the current-voltage curve we consider the intermediate current asymptotics. Essentially this is the regime in which the potential is too small for drift to deplete the charges in the bulk of the semiconductor, yet too large for quasi static equilibrium to dominate the current voltage characteristics. Here it is possible to find analytic solutions to differential equations for the drift diffusion process but the transcendental equations that result from fitting this analytic solution to the boundary data have no explicit analytic solution. As a consequence the results are not easily interpreted, nevertheless we present them here for completeness.

Outer solution (o). Here we look for an asymptotic solution to (3.2) and (3.4) of the form

$$\begin{aligned}\phi^{(o)} &= \log\left(\frac{1}{\delta}\right)\phi_0^{(o)} + \phi_1^{(o)} + \dots, \\ \Phi + \Phi_{bi} &= \log\left(\frac{1}{\delta}\right)\Xi_0 + \Xi_1 + \dots.\end{aligned}$$

To leading order we find

$$\phi_0^{(o)} = \text{constant} = -\frac{\Xi_0}{2}, \quad (3.32)$$

whilst at next order we retrieve the following problem for $\phi_1^{(i)}$:

$$\frac{\partial^3 \phi_1^{(o)}}{\partial x^3} + \frac{\partial \phi_1^{(o)}}{\partial x} \frac{\partial^2 \phi}{\partial x^2} = -2|\hat{J}|, \quad \left. \frac{\partial^2 \phi_1^{(o)}}{\partial x^2} \right|_{x=1} = -N_a \exp\left(\frac{\Phi_{bi}}{2}\right), \quad \phi_1^{(o)}|_{x=1} = -\frac{\Xi_1}{2}. \quad (3.33)$$

In order to couple to this solution to the boundary conditions on $x = 0$ we need to introduce an inner region.

Inner region (i). The inner variable ν is defined by

$$x = \delta^{1/2} \nu$$

such that equations (3.2)-(3.3) now read

$$\frac{\partial^3 \phi}{\partial \nu^3} + \frac{\partial \phi}{\partial \nu} \frac{\partial^2 \phi}{\partial \nu^2} = -2\delta^{3/2} |\hat{J}| \quad \text{in } x > 0, \quad (3.34)$$

$$\phi = 0 \quad \text{and} \quad |\hat{J}| = \frac{\phi_{\nu\nu}^2 - \delta^2 N_a^2}{\phi_{\nu\nu} - \delta\theta} \quad \text{on } \nu = 0, \quad (3.35)$$

We expand ϕ in the inner as follows:

$$\phi^{(i)} = \phi_1^{(i)} + \dots$$

At leading order $\phi_1^{(i)}$ satisfies the problem

$$\frac{\partial^3 \phi_1^{(i)}}{\partial \nu^3} + \frac{\partial \phi_1^{(i)}}{\partial \nu} \frac{\partial^2 \phi_1^{(i)}}{\partial \nu^2} = 0, \quad |\hat{J}| = - \left. \frac{\partial^2 \phi_1^{(i)}}{\partial \nu^2} \right|_{\nu=0}, \quad \phi_1^{(i)}|_{\nu=0} = 0$$

with solution

$$\phi_1^{(i)} = 2 \log \left(1 + \left| \frac{\hat{J}}{2} \right|^{1/2} \nu \right). \quad (3.36)$$

Matching. Taking the large ν limit in (3.36) gives

$$\phi_1^{(i)} \sim 2 \log \nu + \log \left| \frac{\hat{J}}{2} \right| + O\left(\frac{1}{\nu}\right).$$

Writing this in terms of the outer variable $\nu = x/\delta^{1/2}$ gives

$$\phi_1^{(i)} \sim \log \left(\frac{1}{\delta} \right) + 2 \log x + \log \left| \frac{\hat{J}}{2} \right| + O\left(\delta^{1/2}\right). \quad (3.37)$$

Matching to the outer problem at leading order gives

$$\phi_0^{(o)} = 1, \quad \Xi_0 = -2. \quad (3.38)$$

At next order the matching condition (3.37) provides conditions that close (3.33), the outer problem for $\phi_1^{(o)}$

$$\phi_1^{(o)} \sim 2 \log x + \log \left| \frac{\hat{J}}{2} \right| \quad \text{as } x \rightarrow 0.$$

The full outer problem. This is found by combining the above matching condition with (3.33)

$$\frac{\partial^3 \phi_1^{(o)}}{\partial x^3} + \frac{\partial \phi_1^{(o)}}{\partial x} \frac{\partial^2 \phi_1^{(o)}}{\partial x^2} = -2|\hat{J}|, \quad (3.39)$$

$$\left. \frac{\partial^2 \phi_1^{(o)}}{\partial x^2} \right|_{x=1} = -N_a \exp\left(\frac{\Phi_{bi}}{2}\right), \quad (3.40)$$

$$\phi_1^{(o)} \sim 2 \log x + \log \left| \frac{\hat{J}}{2} \right| \quad \text{as } x \rightarrow 0. \quad (3.41)$$

with the correction to the potential being given by the solution to this problem via (3.33c). The exact solution to (3.39), which was independently derived in [11], is

$$\phi_1^{(o)} = 2 \log \left| \beta \text{Ai}(|\hat{J}|^{1/3}(x_1 - x)) + \gamma \text{Bi}(|\hat{J}|^{1/3}(x_1 - x)) \right|,$$

where x_1 , β and γ are arbitrary constants and $\text{Ai}(\cdot)$ and $\text{Bi}(\cdot)$ are Airy functions of the first and second kind, respectively. Requiring that the solution satisfies the matching condition (3.41) the solution determines γ and β so that the solution can be written in the form

$$\phi_1^{(o)} = \log \left| \frac{\hat{J}}{2} \right| + 2 \log \left| \frac{\text{Bi}(|\hat{J}|^{1/3}x_1)\text{Ai}(|\hat{J}|^{1/3}(x_1 - x)) - \text{Ai}(|\hat{J}|^{1/3}x_1)\text{Bi}(|\hat{J}|^{1/3}(x_1 - x))}{|\hat{J}|^{1/3} \left(\text{Ai}(|\hat{J}|^{1/3}x_1)\text{Bi}'(|\hat{J}|^{1/3}x_1) - \text{Bi}(|\hat{J}|^{1/3}x_1)\text{Ai}'(|\hat{J}|^{1/3}x_1) \right)} \right|$$

$\text{Ai}'(\cdot)$ and $\text{Bi}'(\cdot)$ are the derivatives of the Airy functions of the first and second kinds respectively. The final condition (3.40) leads to a, rather complicated, transcendental equation which can be solved to find the final parameter x_1 . The correction to the potential is given by (3.33c) so that in this case

$$\Xi_1 = -2 \log \left| \frac{\hat{J}}{2} \right| - 4 \log \left| \frac{\text{Bi}(|\hat{J}|^{1/3}x_1)\text{Ai}(|\hat{J}|^{1/3}(x_1 - 1)) - \text{Ai}(|\hat{J}|^{1/3}x_1)\text{Bi}(|\hat{J}|^{1/3}(x_1 - 1))}{|\hat{J}|^{1/3} \left(\text{Ai}(|\hat{J}|^{1/3}x_1)\text{Bi}'(|\hat{J}|^{1/3}x_1) - \text{Bi}(|\hat{J}|^{1/3}x_1)\text{Ai}'(|\hat{J}|^{1/3}x_1) \right)} \right|.$$

4. Inclusion of a photo-generated current . Light absorbed in organic photovoltaic diodes produces strongly bound excitation states (electron-hole pairs) that diffuse through the acceptor and the donor until they either recombine, releasing their energy as heat, or meet the acceptor-donor interface, where they can separate (typically in a multi-stage process whose details do not concern us here) into a hole in the donor and an electron the acceptor. We can model this process by including a source term for electrons and holes on the organic-organic interface at $x = 0$ replacing the dimensionless equation (2.13) by

$$[\mathcal{F}_n]_{x=0} = [\mathcal{F}_p]_{x=0} = \frac{J_{\text{phot}}}{q} - R_b(n|_{x=0-}, p|_{x=0+})$$

where J_{phot} is a positive variable representing the contribution to the electric current density from the dissociation of bound excitation states at the interface. On, non-dimensionalising (as in §2.4 with J_{phot} scaling like the current density J), approximating the electron and hole densities in the donor and acceptor, respectively, by zero (as in §2.5), and assuming that the diode is antisymmetric (as in §2.5) this leads

to a modification to the dimensionless-antisymmetric model (2.36)-(2.38) in which (2.37) is replaced by

$$J - J_{\text{phot}} = -\frac{2\delta(p^2|_{x=0} - 1)}{(\lambda^2\theta + p|_{x=0})}. \quad (4.1)$$

Provided $0 < J_{\text{phot}} \ll 1$ and $-\Phi \ll \log(1/\delta)$ the small current asymptotics as expounded in §3.1 are appropriate. In this regime the leading order solution for the potential is independent of the current density and the leading order current density is derived directly from the solution for the leading order potential. In the modified current equation $J - J_{\text{phot}}$ plays the role of the current density in (2.37). It follows that the leading order current density derived from (4.1) is exactly that derived in §3.1 with the addition of J_{phot} so that (3.10) is modified to

$$J \sim J_{\text{phot}} + 4\delta \frac{\sinh(\Phi/2)}{1 + \lambda^2\theta \exp(\Phi/2)}. \quad (4.2)$$

5. Discussion and Conclusions. The asymptotic analysis presented in this paper is successful in predicting analytic relationships for the current-voltage curve of a flat organic semiconducting diode. The curve has three-distinct parts: the low-current part is characteristic of a conventional diode showing current saturation in reverse bias and exponential behaviour in forward bias; the high-current part is dominated by the Ohmic resistance of the bulk, usually interpreted as a series resistance; there is a subtle intermediate-current behaviour that only covers a small range of potentials and currents and which smoothly connects the other two parts. The current-voltage curve displays the same features as the phenomenological Shockley equivalent circuit model, with small shunt resistance (see for example [13]). That is, in reverse bias, it saturates to a constant current, in forward bias it displays exponential behaviour and for very large forward bias the behaviour is linear. As shown in [13] such models can be very successfully fitted to experimental data. For the simple model presented here the ideality factor is always 2. This is a consequence of the recombination law assumed at the interface, which is in our case proportional to charge density. Recombination laws with a different dependence on charge density could be exploited to model different ideality factors.

The diode can act as a photovoltaic device when exposed to radiation of the right wavelengths. This leads to the generation of excitation states (strongly bound electron-hole pairs) which, if they reach the acceptor-donor interface before recombining, can separate into an electron in the acceptor and a hole in the donor and drive an electric current. Typically organic photovoltaics operate in the low-current limit, in which the device lies close to its equilibrium. In this limit the additional photo-generated current J_g has the effect of shifting the current-voltage curve (as plotted in the right panel of figure 3.2) up the J -axis by an amount J_{phot} .

The analysis presented has assumed that the Poole-Frenkel effect is negligible. Notably this effect does not change the small current behaviour since the system is in quasi-equilibrium away from the interface. The Poole-Frenkel term does change the position of the intermediate region of the current-voltage curve and in particular delays the transition to the high-current (and intermediate) limits since it enhances diffusion at high electric fields thus keeping the system near quasi-equilibrium for longer. In the high-current limit the nonlinear resistance encapsulated in the Poole-Frenkel effect leads to a nonlinear current voltage curve that, in the limit of large (negative) applied

voltage Φ , has asymptotic behaviour that depends upon the Poole-Frenkel parameter ν through

$$\log(-J) \sim \nu \left(-\frac{\Phi + \Phi_{bi}}{2} \right)^{1/2} + \frac{\Phi_{bi}}{2}.$$

In fact our analysis points to the interesting observation that it may be possible to use the series resistance part of the current voltage curve to better understand transport in the bulk of the semiconductors.

The analysis performed here forms the basis of an understanding of the behaviour of organic photovoltaic devices. The effects of illumination of the photovoltaic device can be added by including a description of the behaviour of the generation and transport of excitons, as well as their dissociation, into electrons and holes, at the interface. In practice the interface between the donor and acceptor in a photovoltaic device is rarely planar and is typically manufactured with a highly convoluted structure in order to maximise the chance of excitons diffusing there. Nevertheless the fact that, for much of the range of the device its behaviour is dominated by effects occurring in a narrow layer about the interface suggest that, even where this interface is convoluted, analytic progress may be possible. Extending the analysis to account for these and other phenomena remain open questions.

Acknowledgements. JK acknowledges a James Martin fellowship. CPP and JK both acknowledge funding from KAUST via OCCAM. The authors would also like to thank Savina Joseph for her help in preparing the manuscript.

REFERENCES

- [1] Geoffrey B., le Roy P., Prat C., “Organic light-emitting diode (OLED) technology: materials, devices and display technologies”, *Pol. Int.* **55**, 572 (2006).
- [2] Zaumseil J., Sirringhaus H., “Electron and ambipolar transport in organic field-effect transistors”, *Chem Rev* **107**, 1296 (2007).
- [3] Thomas S.W. III, Joly G.D., Swager T.M., “Chemical Sensors Based on Amplifying Fluorescent Conjugated Polymers”, *Chem Rev* **107**, 1339 (2007).
- [4] Gü S., Neugebauer H., Sariciftci N.S., “Conjugated polymer based solar cells”, *Chem Rev* **107**, 1324 (2007).
- [5] Borsenberger P.M., Weiss D., “Organic Photoreceptors for xerography”, Marcel Dekker inc. (1998).
- [6] Stuart B., “Solarmer achieves 8.13 percent OPV efficiency”, *pv magazine* (2007).
- [7] Sze S.M., Kwok K Ng, “Physics of Semiconductor Devices”, 3rd edition, Wiley-Interscience NY, (2006).
- [8] Buxton G.A. and Clarke N., “Modelling the current-voltage characteristics of bilayer polymer photovoltaic devices”. *Phys. Rev. B* **67**, 075205 (2003).
- [9] Barker J.A., Ramsdale C.M. and Greenham N.C., “Computer simulation of polymer solar cells”. *Modelling Simul. Mater. Sci. Eng.* **15**, 13-26 (2007).
- [10] Martin C.M., Burlakov V.M., Assender H.E. and Barkhouse D.A.R., “A numerical model for explaining the role of the interface morphology in composite solar cells”. *J. Appl. Phys.*, **102**, 104506 (2007).
- [11] Brinkman D., Fellner K., Markowich P.A., Wolfram M.-T., “A drift-diffusion-reaction model for excitonic photovoltaic bilayers: asymptotic analysis and a 2-D HDG finite-element scheme” (in preparation).
- [12] Peumans P., Yakimov A. and Forrest S.R., “Small molecular weight organic thin-film photodetectors and solar cells”, *J. Appl. Phys.*, **93**, 3693 (2003).
- [13] Potscavage W.J., Yoo S. and Kippelen B., “Origin of the open-circuit voltage in a multilayer heterojunction organic solar cells”. *Appl. Phys. Lett.*, **93**, 193308 (2008).
- [14] de Jongh P.E. and Vanmaekelbergh D., “Trap-Limited Transport in Assemblies of Nanometer-Size TiO₂ Particles”, *Phys Rev Lett*, **77**, 3427-3430 (1996).

- [15] Pautmeier L., Richert R. and Bässler H., “Poole-Frenkel behaviour of Charge Transport in organic solids with off-diagonal disorder studied by Monte Carlo simulation”, *Synth. Met.*, **37**, 271 (1990).
- [16] Kirkpatrick J., Marcon V., Kremer K., Nelson J., Andrienko D., “Charge mobility in discotic mesophases: a multiscale quantum and classical study”, *Phys Rev Lett*, **98**, 227402 (2007).
- [17] Tansae C., Blom P.W.M., de Leeuw D.M. and Meijer E.J., “Charge carrier density dependence of mobility in poly(p-phenylene vinylene)”, *Phys. Stat. Sol. B*, **201**, 1236 (2004).

RECENT REPORTS

38/11	Ice-lens formation and con nment-induced supercooling in soils and other colloidal materials	Style Cocks Peppin Wettlaufer
39/11	An asymptotic theory for the re-equilibration of a micellar surfac- tant solution	Griffiths Bain Breward Chapman Howell Water
40/11	Higher-order numerical methods for stochastic simulation of chemical reaction systems	Székelý Burrage Erban Zygalakis
41/11	On the modelling and simulation of a high pressure shift freezing process	Smith Peppin Ángel M. Ramos
42/11	An efficient implementation of an implicit FEM scheme for fractional-in-space reaction-diffusion equations	Burrage Hale Kay
43/11	Coupling fluid and solute dynamics within the ocular surface tear film: a modelling study of black Line osmolarity	Zubkov Breward Gaffney
44/11	A prototypical model for tensional wrinkling in thin sheets	Davidovitch Schroll Vella Adda-Bedia Cerde
45/11	A fibrocontractive mechanochemical model of dermal wound clo- sure incorporating realistic growth factor	Murphy Hall Maini McCue McElwain
46/11	A two-compartment mechanochemical model of the roles of trans- forming growth factor β and tissue tension in dermal wound heal- ing	Murphy Hall Maini McCue McElwain
47/11	Effects of demographic noise on the synchronization of a metapop- ulation in a fluctuating environment	Lai Newby Bressloff
48/11	High order weak methods for stochastic differential equations based on modified equations	Abdulle Cohen Vilmart Zygalakis
49/11	The kinetics of ice-lens growth in porous media	Style Peppin

52/11	Image Inpainting based on coherence transport with Adapted distance functions	März
53/11	Surface growth kinematics via local curve evolution	Moulton Goriely
54/11	A multiple scales approach to evaporation induced Marangoni convection	Hennessey Münch
55/11	The dynamics of bistable liquid crystal wells	Luo Majumdar Erban
56/11	Real-Time Fluid Effects on Surfaces using the Closest Point Method	Auer Macdonald Treib Schneider Westermann
57/11	Isolating intrinsic noise sources in a stochastic genetic switch	Newby
58/11	Riemann-Cartan Geometry of Nonlinear Dislocation Mechanics	Yavari Goriely
59/11	Helices through 3 or 4 points?	Goriely Neukirch Hausrath
60/11	Bayesian data assimilation in shape registration	Cotter Cotter Vialard

Copies of these, and any other OCCAM reports can be obtained from:

**Oxford Centre for Collaborative Applied Mathematics
Mathematical Institute
24 - 29 St Giles'
Oxford
OX1 3LB
England
www.maths.ox.ac.uk/occam**